Efficient integration of plug-in electric vehicles via reconfigurable microgrids

Abdollah Kavousi-Fard, Amin Khodaei[*]

Department of Electrical and Computer Engineering, University of Denver, Denver, CO 80210, USA

A R T I C L E   I N F O

A B S T R A C T

This paper investigates the viability of the reconfigurable microgrids (RMGs) in facilitating the integration of plug-in electric vehicles (PEVs). The reconfiguration ability of microgrids, which is enabled by the use of remotely controlled switches (RCSs), will support the high penetration of PEVs and renewable distributed generators (DGs) while reducing the total operation cost and potentially enhance microgrid reliability. The objective of the proposed optimal scheduling problem is to minimize the total cost of power supply by distributed energy resources (DERs) and upstream network energy exchange, battery degradation cost in PEVs, cost of switching during the reconfiguration, and expected customer interruption costs as a reliability index. To address the high level of the uncertainties in the problem, a scenario-based stochastic framework is devised to capture the uncertainties associated with the charging and discharging values of PEVs, number of PEVs in each fleet, time of the daily trips for PEVs, hourly load consumption, hourly output power of renewable DGs, and hourly market price. The satisfying performance and merits of the proposed model are examined on a test microgrid.

© 2016 Elsevier Ltd. All rights reserved.

1. Introduction

A Microgrid is defined as a group of interconnected loads and distributed energy resources (DER) which can operate either connected to or disconnected from the utility grid [1], and accordingly improve the quality of the electrical services to local customers from both operation and reliability points of view [2,3]. Some of the major benefits of microgrid deployments can be listed as fewer customer interruptions and improved reliability, lowered emissions, higher power quality, reduced operation costs, and higher efficiency [4,5]. These promising features have resulted in initiating significant research on the microgrids operation, control, and planning in recent years. In [6], an optimization framework based on the matrix real-coded genetic algorithm is suggested to investigate the optimal operation of a microgrid. The proposed method consists of a forecasting module, an energy storage system, and an optimization approach. In [7], a method based on linear programming is presented to decrease the cost of a hybrid solar-wind microgrid with regards to the environmental constraints. In [8], authors assess the optimal fuel consumption management problem

in a microgrid for supplying the electrical/thermal energy demands with minimum reserve power. Four different power-sharing schemes are considered among the power sources in the microgrid to solve the problem. In [9], the interactive effects of a grid-connected microgrid are assessed to see the microgrid master controller's role in optimal operation of the microgrid. Similarly, the daily operation management of a microgrid including a wind turbine (WT) and a distributed energy storage (DES) for minimizing the microgrid costs are addressed in Ref. [10].

As it can be inferred from these works, and many other available works on microgrid scheduling, the main focus of the researchers for improving the microgrid operational viability has been on the optimal scheduling of the energy resources within the microgrid (DGs and DES) as well as interactions with the utility grid. However, one of the most useful, and yet less studied, strategies that can greatly enhance the microgrid's operational viability is the network reconfiguration. By definition, reconfiguration is the process of changing the topology of the network using some remotely controlled switches (RCSs) [11]. This process is implemented by the use of pre-located sectionalizing switches (normally closed switches) and tie switches (normally open switches) on the feeder end points. The positive effect of optimal reconfiguration on the network power losses is investigated using different methods such as brute-force approach [12], neural network [13], optimum flow

* Corresponding author. University of Denver, Denver, CO, 80210, USA.
  E-mail address: amin.khodaei@du.edu (A. Khodaei).

Nomenclature

Indices

e	index for scenario
g	index for element of a scenario
i	index for DER
j	index for branch
m,n	index for bus
s	index for switching
t	index for time
v	index for PEV fleet
z	index for discharge of battery
min/max	superscript for minimum/maximum value

Parameters

a,b	Wöhler curve parameters
$C^{Rel/PEV/Sub/DER/SW/d}$	cost of reliability/PEVs/main. grid/DERs/ Switching/degradation
C^{bat}	battery investment cost ($)
c	hourly price of energy purchased from DERs
c^{PEV}	hourly price of V2G
c^{M}	hourly price of main grid
La	average load connected to bus
$N_{U/B/Br}$	number of uncertain variables/buses/branches
N_{DER}	number of DER units including MTs and FCs
$N_{v/L/SW}$	total number of PEVs/loops/switches
$N_{dis/c}$	number of discharge/life cycles
N_s	number of scenarios after scenario reduction
T	planning horizon
w	number of random variables in the problem

Y/θ	magnitude/phase of line impedance
γ^{I}/γ^{F}	initial/final DoD in a discharge cycle.
λ	failure rate of the component.
λ^{RCS}	hourly switching price.
η^{c}/η^{d}	charging/discharging efficiency.
Δt	planning time interval.

Variables

$Cost$	total microgrid cost.
E^{bat}	usable energy of the battery (kWh).
E^{D}	energy for PEVs in fleet to drive.
E	energy in batteries of fleet.
E^{ini}/E^{fin}	initial/final energy in PEV fleet.
DT	distance between scenarios.
f_s	optimal function value for scenario s.
N^{RCS}	number of switching operation.
P	output power of DER
P^{M}	hourly/max imported power from main grid.
$P^{c}/P^{d}/P^{I}$	charge/discharge/idle capacity of PEV fleet.
P^{PEV}	charge/discharge rate of PEV fleet.
P^{Inj}/Q^{Inj}	hourly injected active/reactive power at bus.
pr	probability of an element in a scenario.
R	a possible scenario of the problem.
S^{L}	power flow in the feeder
t'	time in which SOC is set to a specific value.
U	status of grid connection of fleet.
$U^{c}/U^{d}/U^{I}$	indicator of fleet in charge/discharge/idle mode.
V/δ	voltage magnitude/phase of bus.
ξ_s	set of scenarios
β	on or off status of switch.

pattern [14], graph theory [15], heuristic techniques [16], expert systems [11], ant colony optimization algorithm [17] and hybrid simulated annealing algorithm [18]. The benefit of reconfiguration on other objectives such as enhancing load balance [19], improving voltage profile [20], reducing total system cost [21] and enhancing system reliability [22] are further discussed in the literature. However, the important role of reconfiguration in improving microgrid's operational viability is still an untapped area of research. The limited research in this area in conducted by Nafisi et al. [23] which has used the reconfiguration strategy for reducing the cost of energy losses in the microgrid. However, neglecting renewable DGs as well as their associated uncertainty, are one of the main deficiencies of this work. In addition, the objective function only considers the cost of energy supplied by the microgrid and neglects the reliability reinforcement ability of the reconfiguration. In [24], reconfiguration strategy is employed for minimizing the total vulnerability of the microgrid. The simulation results on the IEEE 38-bus test system show that the proposed assessment system based on the reconfiguration strategy can effectively enhance the microgrid operation. Here again significant advantages of reconfiguration for reducing the total network costs are neglected. In [25], the system reconfiguration was considered for microgrids in the presence of renewable DGs and load forecast errors. The problem is formulated as a single-objective optimization problem to minimize the cost of power losses, the cost of power drawn at the point of common coupling (PCC), and the cost of power supplied by dispatchable DGs. While valuable, ignoring the cost of switching, different types of renewable DGs, and the impact of the reconfiguration on the supply reliability are of noticeable deficiencies.

This paper investigates the optimal reconfiguration of microgrids considering dispatchable DGs, Plug-in Electric Vehicles (PEVs), and a high penetration of renewable DGs. A stochastic cost-based optimization framework is proposed to determine the optimal switching scheme in the microgrid when scheduling available resources as well as the interactions with the utility grid. To diminish the high charging effects of PEVs, the idea of Vehicle-2-Grid (V2G) within the microgrid is employed. Technically, PEVs are hourly distributed in the microgrid and may be considered as mobile demands or mobile energy storage units [26]. The optimal management of these resources can offer benefits for the microgrid including shifting the peak load, reducing the power loss, and lowering the total operation cost [27] in addition to known benefits to the entire grid in terms of emission reduction [28]. The inclusion of renewable DGs and PEVs, however, would inject significant uncertainty to the microgrid that may affect operation and planning processes. In order to solve this issue, a scenario-based stochastic method is used to model the uncertainties associated with the active and reactive loads, output power of wind turbine (WT) and photovoltaic's (PV) as common types of renewable DGs, utility grid energy price, departure and arrival times of PEVs, state of charge of batteries (SOC) in PEVs, and the number of PEVs in each considered fleet. Analysis is performed on the IEEE 32-bus test system, incorporating a PV, two WTs, a Fuel Cell (FC), two Micro Turbines (MT) and three PEV fleets, as well as 5 normally open switches and 32 normally closed switches, to show the merits and the effectiveness of the proposed model. The main contributions of the paper can be summarized as follows: 1) investigation of the impacts of the reconfiguration strategy on microgrid optimal operation under

uncertainty, 2) development of an efficient formulation for optimal operation and management of reconfigurable microgrids with high penetration of renewable energy sources and PEVs and 3) introduction of a smart charging and discharging strategy for PEVs in reconfigurable microgrids using the V2G technology.

The rest of this paper is organized as follows: Section II explains the reconfiguration strategy and PEV technology in microgrids. In Section III the formulation of the proposed stochastic problem is explained. Section IV describes the scenario-based approach for modeling the uncertainty. The simulation results on a typical microgrid are given in Section V. Finally, the main concepts and conclusions of the work are provided in Section VI.

2. Reconfigurable microgrids (RMG)

2.1. Reconfiguration strategy

Reconfiguration strategy is realized as an operation for altering the topology of the feeders in distribution networks, which is implemented by using tie and sectionalizing switches. Reconfiguration strategy can benefit the distribution operator by providing a fast solution for enhancing the reliability, reducing power losses, improving the power quality, and decreasing the distribution feeder congestion. In addition to these benefits, a timely reconfiguration can restore the undamaged parts of the microgrid under emergency conditions and also support the increased penetration of renewable DGs and PEVs by clearing the feeder congestion and dividing equal loads on different feeders. According to practical experiments, reconfiguration strategy can potentially result in up to 30% annual reduction in the average outage duration for the overhead feeders of a well-maintained distribution network [23]. In order to consider the reconfiguration strategy in the microgrid, remote meter readings for voltage and current parameters should be provided in the microgrid master controller. The microgrid master controller will conduct the reconfiguration and determine the optimal topology of the microgrid distribution network. To successfully perform this task, however, the microgrid needs to be equipped with a high speed communication infrastructure (for communicating data from different parts of the microgrid including the measurement devices, protective devices, and actuators to the master controller and further transmitting controlling commands) as well as controllable switches (which can be either manual switches or RCS) to alter the microgrid topology.

2.2. PEV technology

In recent years, the increasing concerns about the high amount of greenhouse gas emissions by vehicle fleets has supported the idea of replacing the traditional combustion engine vehicles with more efficient and cleaner electric vehicles, and in particular, PEVs. A PEV is any motor vehicle that can be charged from an external source of electricity. In the view of the electric companies, a number of PEVs especially in the form of a fleet can be supposed as dispersed movable loads that should be managed to avoid any problem in supplying the electricity to consumers. Without an appropriate scheduling, PEVs charging demand can become troublesome creating feeder congestion or even long interruptions. In order to tackle this issue, some assumptions are made to model the behavior of PEVs. The PEV fleet characteristics are determined by their departure time, arrival time, and the departure location and destination. By knowing the fleet characteristics and the expected number of PEVs in the fleet, its main features such as state of charge (SOC); (the ratio of available energy to maximum storable energy in the battery), energy consumption, and min/max capacity could be determined. According to recent reports, an average driver makes two main trips per day with some short trips up to 10 min [29]. In the hourly scheduling plan, the short trips can be ignored. Therefore, there would be a daily travel for each PEV from a starting location at the beginning of the day and then a return to the same point at the end of the trip. Consequently, the amount of energy used in the travel path equals that in the return path [30]. It is reported that the average annual driving distance of a PEV fleet is 12,000 miles with an average of 32.88 miles per day [31]. Considering the daily energy consumption of 9 kWh for each PEV, the average energy of 3.65 kWh is consumed per mile. In order to make the modeling process more practical, the PEV battery at the beginning of the first trip is assumed fully charged i.e., SOC is 100%. During the hours that PEV is in the charging location, either at parking or at home, the V2G technology is used to provide a bidirectional power exchange between the PEV and the grid. PEVs can charge/discharge from/to the grid based on the microgrid operation cost and battery limitations such as charge/discharge rate and Depth of Discharge (DoD).

3. Problem formulation

The microgrid optimal scheduling problem is formulated as a constrained single-objective optimization problem. In the proposed optimization problem, the control variables consist of 1) hourly on/off status of sectionalizing and tie switches; 2) optimal output power of DERs including FC and MT; 3) hourly charge/discharge/idle states of the PEV fleet; 4) amount of power exchanged between PEV fleet and microgrid, through either charging or discharging, and 5) amount of power exchanged between the microgrid and the main grid.

3.1. Objective function

The objective is to minimize the microgrid total operation cost incorporating cost of switching, cost of power generation by dispatchable DERs, cost of charging PEVs, cost of reliability, and cost of power purchase from the main grid (1).

$$\text{Min} \quad Cost = C^{SW} + C^{DER} + C^{PEV} + C^{Rel} + C^{Sub} \tag{1}$$

Cost terms are explained as follows:

$$C^{SW} = \sum_{t=1}^{T} \sum_{s=1}^{N_{SW}} N_s^{RCS} \lambda^{RCS} \tag{2}$$

$$C^{DER} = \sum_{t=1}^{T} \sum_{i=1}^{N_{DER}} c_{it} P_{it} \tag{3}$$

$$C^{PEV} = \sum_{t=1}^{T} \sum_{v=1}^{N_v} c_{vt}^{PEV} P_{vt}^{PEV} + \sum_{z=1}^{N_{dis}} C_z^d \left(\gamma^I, \gamma^F \right) \tag{4}$$

$$\sum_{z=1}^{N_{dis}} C_z^d \left(\gamma^I, \gamma^F \right) = \sum_{z=1}^{N_{dis}} C_z^d \left(0, \gamma^F \right) - C_z^d \left(0, \gamma^I \right) \tag{5}$$

$$C_z^d (0, \gamma^s) = \frac{C^{bat} \times \gamma^s \times E^{bat}}{N^c(\gamma^s)} \tag{6}$$

$$C^{Rel} = \sum_{j=1}^{N_{br}} ECOST_j = \sum_{j=1}^{N_{br}} La_j c_j^L \lambda_j \tag{7}$$

$$C^{Sub} = \sum_{t=1}^{T} c_t^M P_t^M \tag{8}$$

The switching cost is defined in (2) which models the aging process of switches in the reconfiguration. The value assigned to the state of each RCS can be 0 or 1 showing open and closed state of that switch, respectively. The value of N_s^{RCS} is calculated later in (15). Cost of power supplied by DERs is represented by (3) which calculates the cost of power produced by DERs, either renewable DGs or fuel-based DGs (FC and MT). The PEV cost (4) contains two parts: 1) cost of energy for charging/discharging of PEV and 2) cost of using V2G technology represented in terms of battery degradation. The battery degradation cost is a result of the extra cycling of battery during the V2G technology and is calculated by Wöhler curve [30]. Fig. 1 shows Wöhler curve for a typical battery. As DoD is increased, the number of cycles to battery failure is decreased. Wöhler curve is formulated as $N^c(\gamma) = a.\gamma^b$ [30], where, parameters a and b are obtained based on the battery type. By the use of the above equation, the battery degradation cost from initial status of γ^I to γ^f is determined in (5). Here the battery degradation cost from fully charged status to a specific DoD value γ^s is calculated as in (6). In order to consider the effect of reliability improvement in the formulation, the expected customer interruption cost (ECOST), as a commonly used reliability index, is considered in the objective function to form the reliability cost (7). This term measures the expected economic losses caused by any interruption in the energy supply. It is shown in the literature that this index can help planners to confirm the adequate level of reliability for electric customers, grant economic justification for determining the network reinforcement and redundancy allocation, recognize weak points in the system, establish suitable maintenance scheduling, and develop proper operation policies [32]. In (7), the price of interruption at each bus is calculated using the composite customer damage function (CCDF) [22]. Finally, the main grid cost (8) considers the cost of power purchased from the main grid in the grid-connected mode.

3.2. Problem constraints

The proposed objective is subject to the following operational constraints:

$$P_i^{min} \leq P_{it} \leq P_i^{max} \tag{9}$$

Fig. 1. Wöhler curve for lithium-ion battery.

$$P_{mt}^{Inj} = \sum_{n=1}^{N_B} V_{mt} V_{nt} Y_{mn} \cos(\theta_{mn} + \delta_{mt} - \delta_{nt}) \tag{10}$$

$$Q_{mt}^{Inj} = \sum_{n=1}^{N_B} V_{mt} V_{nt} Y_{mn} \sin(\theta_{mn} + \delta_{mt} - \delta_{nt}) \tag{11}$$

$$V_n^{min} \leq V_{nt} \leq V_n^{max} \tag{12}$$

$$\left| P_t^M \right| \leq P^{M,max} \tag{13}$$

$$S_t^L \leq S^{L,max} \tag{14}$$

$$N_s^{RCS} = \sum_{t=1}^{T} |\beta_t - \beta_{t-1}| \tag{15}$$

$$N_s^{RCS} \leq N^{RCS,max} \tag{16}$$

$$U_{vt}^c + U_{vt}^d + U_{vt}^l = U_{vt} \tag{17}$$

$$U_{vt} P_v^{c,min} \leq P_{vt}^c \leq U_{vt} P_v^{c,max} \tag{18}$$

$$U_{vt} P_v^{d,min} \leq P_{vt}^d \leq U_{vt} P_v^{d,max} \tag{19}$$

$$E_{vt} = E_v^{ini} + \sum_{l=1}^{t} \left(U_{vt}^c P_{vl}^c \eta_v^c - U_{vt}^d P_{vl}^d \eta_v^d \right) - \sum_{l=1}^{t} (1 - U_{vl}) E_{vl}^D \tag{20}$$

$$P_{vt} = \frac{\left(E_{vt} - E_{v(t-1)} \right)}{\Delta t} \tag{21}$$

$$E_v^{min} \leq E_{vt} \leq E_v^{max} \tag{22}$$

$$E_v^{fin} = E_v^{ini} \tag{23}$$

$$E_v^{t'} = E_v^{max} \tag{24}$$

$$N_L = N_{Br} - N_B + 1 \tag{25}$$

where (9) limits the DG generation capacity, (10) and (11) represent the AC power flow constraints for supplying active and reactive loads, (12) represents the voltage limitation on buses, (13) determines the maximum power exchange between the microgrid and the upstream network, (14) imposes thermal limit for feeders, (15) calculates the number of switching in the microgrid and (16) limits the maximum number of switching actions during the reconfiguration. In (17), the hourly charge/discharge/idle states of fleets are determined. Once PEVs are connected to the main grid, their charge, discharge or idle status should be determined optimally. Here, the parameter $U_{v,t}$ shows the presence of PEV fleet v in the charging location at time t. Once $U_{v,t} = 0$, the PEV fleet is not connected to the grid and once $U_{v,t} = 1$ it means that PEV fleet is connected, i.e., either charging, discharging or idle mode. Constraints (18) and (19) show the maximum/minimum charge and discharge power rates, respectively. Constraint (20) represents the hourly energy balance in PEV batteries and (21) shows the amount of power charged or discharged in each PEV fleet. Since the
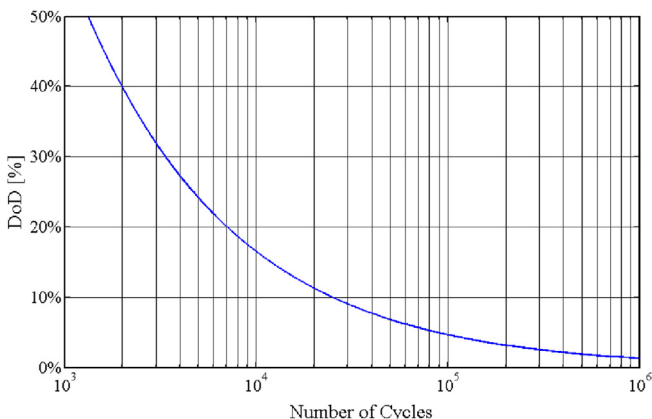
scheduling time resolution is assumed to be 1 h, Δt is considered to be 1 in this equation. Constraint (22) shows the minimum and maximum energy limits of each PEV fleet. The final SOC of each PEV fleet at the end of the day should equal its initial SOC at the beginning of the day as shown in (23). The SOC of PEV at the beginning of the first trip is determined by (24). The PEV battery is assumed to be fully charged before the first trip at the beginning of the day. Finally, the radial structure of the network is preserved using (25). During the optimization process and after each switching, Depth-First Search (DFS) algorithm [33] is employed to find the loops formed in the network. This algorithm counts the number of loops (cycles), using (25), and once a loop is detected, a tie or sectionalizing switch is opened in that loop to make the network radial.

4. Modeling uncertainties based on scenario generation

The proposed optimal scheduling problem consists of a high number of uncertain parameters including charge/discharge pattern of PEVs, active and reactive loads, electricity price, WT/PV output power, number of PEVs in each fleet, and arrival and departure time of PEV fleets. In order to model the effect of the uncertainties, a scenario-based stochastic framework is devised in this section.

4.1. Scenario generation

In the proposed method, each uncertain parameter is replaced by an appropriate probability density function (PDF). Each PDF domain is divided into several slices or probability levels. Each probability level represents a specific forecast/modeling error in the associated uncertain parameter. Fig. 2 shows a normal PDF with seven probability levels.

The process of scenario generation is based on the use of roulette wheel mechanism (RWM). In each scenario and for each uncertain parameter, a random number in the range [0,1] is produced. This random number falls in one of the probability levels of the associated PDF which shows the probability of existence of some error in the uncertain variable. This process is repeated for all uncertain variables to generate a complete scenario.

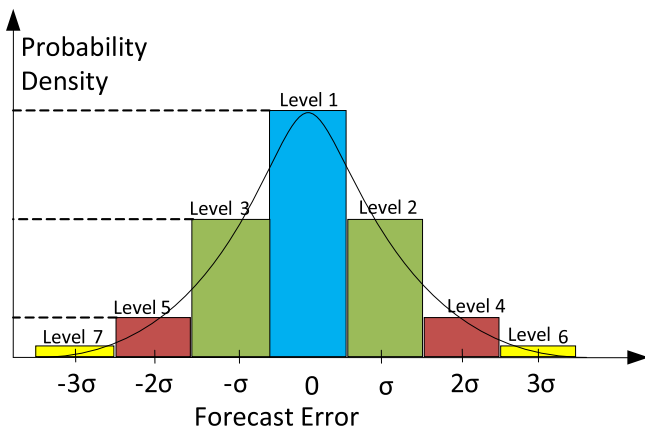$$R_e = [r_{e1}, r_{e2}, r_{e3}...., r_{ew}]$$ (26)

Fig. 2. Normal PDF function with seven probability levels.

4.2. Scenario reduction & aggregation

Initially, a large number of scenarios are randomly generated. However, the scenario set should be reduced to alleviate computation requirements. A number of different scenario reduction methods are introduced in the literature [34]. This paper employs the simultaneous backward method due to its low computational effort and high accuracy. This method calculates the distance between different scenarios to select the most dissimilar and probable scenarios. The following steps are employed to reduce the scenarios:

Step 1: Consider ξ_s as the initial set of the scenarios. Also suppose DS as the set of remained scenarios after scenario reduction process which is initially empty. Compute the distance between any two scenarios as follows:

$$DT_{ee'} = DT(R_e, R_{e'}) = \sqrt{\sum_{g=1}^{w} (r_{eg} - r_{e'g})^2} \quad e, e' = 1, 2, ..., N_S$$ (27)

Step 2: Determine the least distance with other scenarios for each scenario R_e:

$$DT_{el} = \min DT_{ee'} \quad e, e' \in N_s; e' \neq e$$ (28)

where l holds the number of scenarios with the least distance from scenario s.

Step 3: Multiply the probability of each scenario pr_e with the least distance from other scenarios:

$$PD_{e'l} = pr_l \times DT_{e'l} \quad e' \in N_s$$ (29)

Step 4: Omit the dth scenario with the lowest value for the below criterion from the initial scenarios set ξ_s:

$$PD_d = \min PD_e \quad e \in N_s$$ (30)

$$\xi = \xi - \{d\}, \quad DS = DS + \{d\}, \quad pr_l = pr_l + pr_d$$ (31)

Step 5: Repeat Steps 2 to 4 until reaching the desired number of scenarios.

The above scenario reduction procedure will omit similar scenarios as well as scenarios with low probabilities. The remained scenario set is therefore diverse enough to model the maximum uncertainty spectrum for the problem.

Each scenario would create a deterministic-equivalent framework of the stochastic problem. The optimal solutions of different scenarios are combined together via an aggregation process to construct the final optimal solution:

$$f = \sum_{e=1}^{N_S} \frac{\prod_{g=1}^{w} pr_{eg}}{\sum_{e=1}^{N_S} \prod_{g=1}^{w} pr_{eg}} \times f_w$$ (32)

This equation determines a single optimal solution for the stochastic problem than a set of solutions. By using this aggregation process, not only the interpretation of each single scenario becomes
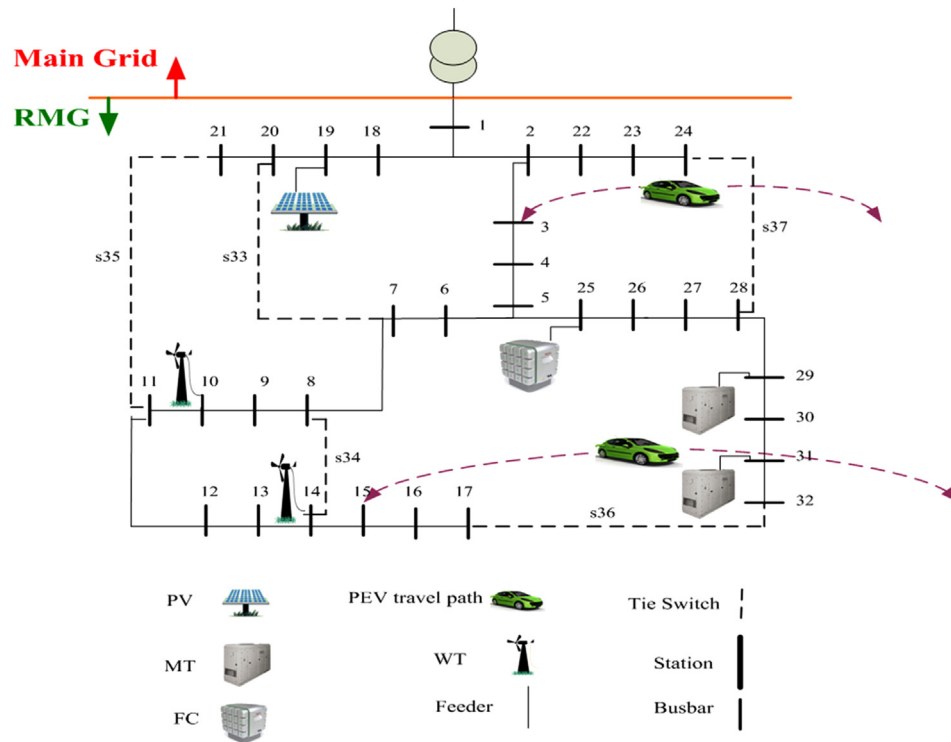
Fig. 3. Schematic of the RMG with DERs and PEV fleet.

possible, but also the structure of the original stochastic problem is preserved.

5. Simulation results

The proposed model is examined on the IEEE 32-bus test system [35] as a test microgrid (Fig. 3). The microgrid distribution network includes 5 tie switches shown by dotted lines and 32 sectionalizing switches shown by solid lines. There is a main circuit breaker at PCC and a sectionalizer at the beginning of each feeder. The microgrid includes different types of DGs, including two WTs, one PV, one FC and two MTs. The DGs characteristics are shown in Table 1. Similar power curves are considered for both WTs, as they are assumed to be in close proximity, while the output power of WT 2 is assumed to be 1.2 times of the power production of WT 1 due its larger size. The normalized forecast output power curve of WTs and PV sources are depicted in Figs. 4 and 5. Figs. 6 and 7 show the RMG aggregated load demand and market energy price at different hours of the day, respectively. Regarding PEVs, two EV fleets with different capacities and routs are considered in the microgrid. Table 2 shows the number of PEVs in each fleet and the information of each trip. The capacity of each PEV fleet is shown in Table 3. In order to make the

analysis more practical, it is assumed that parts of EV fleets' travels occur outside of the microgrid; either the destination or the arrival location. Therefore, the microgrid master controller would schedule the charge/discharge of PEVs at hours that PEVs are inside the microgrid boundaries. It is clear that full inside travels can be considered in a similar way. According to the high dominant market of batteries, lithium-ion with Wöhler curve parameters of $a = 1331$ and $b = -1.825$ are considered for PEVs and the battery investment cost is assumed to $315 [36]. In this work, 80% DOD is considered to avoid high battery aging.

The optimization problem is solved using the SAMCSA algorithm introduced in Ref. [22]. The population size of algorithm is 25 and the termination criterion is 100 iterations. The stochastic framework models the uncertainties of forecast error in charge/discharge pattern of PEVs, active and reactive load, electricity price, WT/PV output, number of PEVs, and arrival and departure time of PEVs using normal PDF for all variables. The normal PDF with seven probability levels are shown in Fig. 2. It is clear that any other PDF can be used for modeling the uncertainty of the problem in the same manner as described in the paper. To model the uncertainty effect, 1000 different scenarios are generated initially which are reduced to 20 most probable and dissimilar scenarios after scenario

Table 1
The limitations and energy price of DGs.

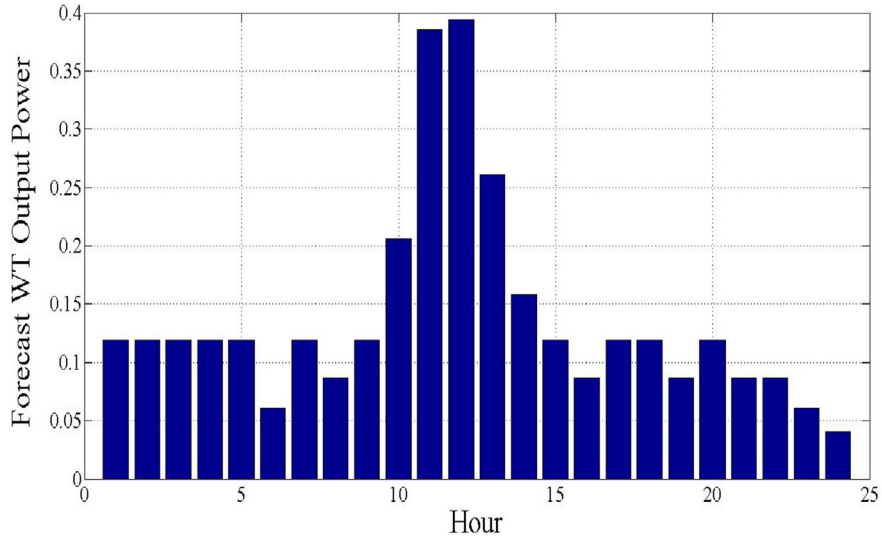| Type	Min power (kW)	Max power (kW)	Price ($/kWh)	Start-up/Shut-down cost ($)
WT-1	–	1500	–	–
WT-2	–	1800	–	–
PV	–	2000	–	–
FC	80	1000	0.294	1.65
MT-1	100	1500	0.457	0.96
MT-2	100	1500	0.457	0.96

Fig. 4. Normalized forecasted WT power generation.
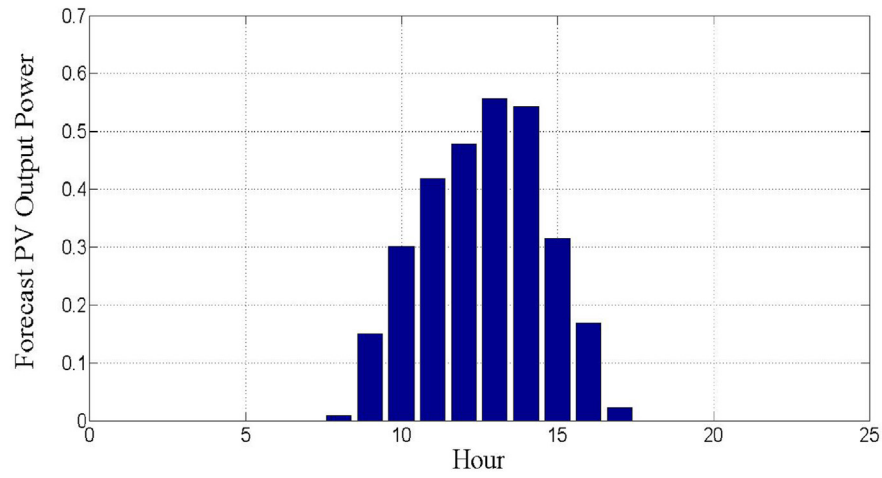

Fig. 5. Normalized forecasted PV power generation.
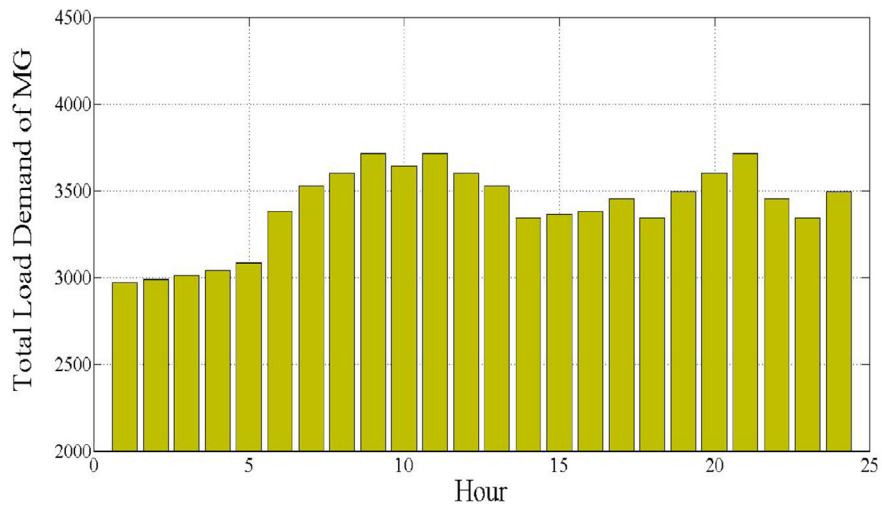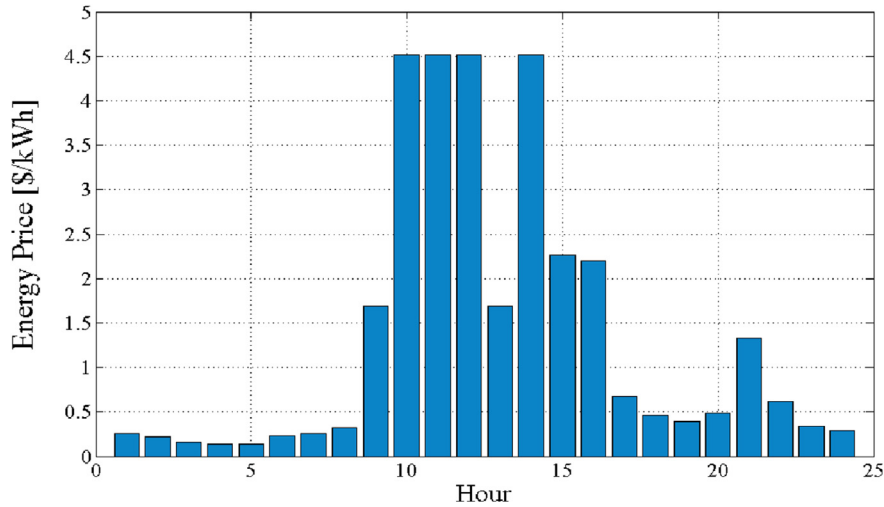

Fig. 6. Total load demand of the RMG.

Fig. 7. Hourly forecast energy price.

Table 2
PEV fleet travel characteristics.

Fleet number	First trip				Second trip			
	Departure		Arrival		Departure		Arrival	
	Time	Bus	Time	Bus	Time	Bus	Time	Bus
1	6:00	3	7:00	OMG*	17:00	OMG	18:00	3
2	7:00	OMG	8:00	15	18:00	15	19:00	OMG

*Outside of microgrid (OMG).

Table 3
PEV fleet characteristics.

Fleet number	Capacity (kWh)		Charge/Discharge rate (kW)	
	Min	Max	Min	Max
1	263	1973	7.3	496
2	219	1644	7.3	292

reduction. This reduction shows a filtering ratio of 1000/20 = 50. It is clear that the filtering ratio can be reduced to capture more uncertainty spectrum but with the cost of higher computational burden. As for the switching, assuming the total life expectancy of 30 years and a long interrupting life of up to 150,000 operations for each RCS [37], the maximum daily switching operations of each RCS is computed as 18, among which 16 operations are devoted to the reconfiguration and 2 operations are designated for fault detection, isolation, or maintenance outages.

The microgrid optimal scheduling problem is solved for a 24-h period. The uncertainties associated with the forecast error of WT and PV output power, active and reactive loads, departure and arrival times of the PEVs fleets, SOC of batteries, number of PEVs in a fleet and energy price are modeled using the proposed scenario-based approach. In order to understand the effect of each element individually, four cases are defined:

Case 1: Microgrid scheduling considering DERs (dispatch only) and neglecting PEVs and Reconfiguration.
Case 2: Microgrid scheduling considering DERs and neglecting PEVs and Reconfiguration.

Case 3: Microgrid scheduling considering DERs and PEVs and neglecting Reconfiguration.
Case 4: Microgrid scheduling considering DERs, PEVs, and Reconfiguration.

Table 4 shows the comparative cost of the microgrid for different scenarios. According to the results of scenario one and two, it is deduced that allowing the dispatchable DGs to shut-down at some hours can reduce the total cost of the microgrid properly. This issue mainly roots in the high cost of power generation by some DGs in comparison with the market price at the same hours. Therefore, DGs ability to switch between On/Off can provide more flexibility for the microgrid to reduce its operation costs. For the rest of scenarios, this authority is considered for DGs. From scenarios two and three, it is seen that the existence of PEVs in the microgrid could reduce the operation costs. In other words, while it

Table 4
Expected cost function value in different scenarios.

Hour	Cost function value (€ct) × 10^3			
	Scenario 1	Scenario 2	Scenario 3	Scenario 4
1	0.9846	0.9426	0.9322	0.9314
2	0.9962	1.0385	0.9334	0.9322
3	0.8790	0.8057	0.8144	0.8113
4	0.8345	0.7552	0.8117	0.8105
5	0.8402	0.7610	0.8176	0.8156
6	0.9397	0.8851	0.9826	0.9758
7	1.2255	1.1798	1.1756	1.1532
8	1.4951	1.3223	1.3181	1.3082
9	2.5709	2.5874	2.5942	2.5777
10	3.5862	3.6352	3.8669	3.7416
11	4.3970	4.4816	4.3177	4.2718
12	4.6776	4.6925	4.6879	4.6667
13	4.4800	4.5724	4.4914	4.4823
14	4.2447	4.2492	4.1983	4.1614
15	3.1265	3.1685	3.1800	3.1280
16	2.4359	2.4456	2.7683	2.6920
17	1.8119	1.8162	1.7057	1.7011
18	1.5657	1.5623	1.6243	1.6184
19	1.4365	1.4209	1.4167	1.4167
20	1.7223	1.7217	1.6015	1.6008
21	1.8859	1.8705	1.5980	1.5000
22	1.6519	1.6711	1.4201	1.4190
23	1.2235	1.2053	1.1968	1.1939
24	1.1006	1.0644	1.0602	1.0599
Total	50.1119	49.8550	49.5136	48.9695

might be expected first that supplying PEVs' charging demand would be new load for the microgrid and thus can increase the total costs; but V2G idea has even reduced the daily cost of the microgrid. Consequently, this technology will support the high penetration of PEVs in the microgrid. Finally, the last scenario considers the reconfiguration of feeders in the microgrid. According to the simulation results, the reconfiguration strategy could reduce the total microgrid costs effectively. This reduction is achieved without any additional cost and just through the reconfiguration of the microgrid.

Table 5 shows the results of optimal power dispatch of DGs in scenario 4. According to these results, FC and MTs are forced to shut down at the first hours of the day to reduce the microgrid costs. Instead, it is preferred to reduce the amount of power injection from the up-stream network at mid-day hours by increasing the power production of DGs. Table 6 shows the optimal amount of hourly energy charged/discharged by PEVs.

This is a realistic constraint which should be considered in the formulation. Also, it is supposed that there would be 50% energy remained in PEV battery when entering or quitting the microgrid during the day (except in the first exit in the morning which is fully charged). According to these results, PEVs of the first fleet tend to discharge at the last hours of the day. On the other hand, they intend to be charged during the first hours of the day when the energy market is cheaper. Note it that PEVs can reduce the total cost by storing energy in one bus with/without transferring the stored energy to the other buses. Similar behavior can be seen for the second PEV fleet. The last column of Table 6 shows the status of open switches after reconfiguration of the microgrid.

Fig. 8 shows the 24-h total power loss for different scenarios. For better comparison, the initial amount of network power loss is also shown. According to this figure, the application of DGs in the microgrid has caused the most reduction in power loss, as they can be used to locally supply loads. Optimal operation and management of DGs during the 24-h time horizon can further effectively reduce operation costs. However, the penetration of PEVs in the microgrid increases the total power loss as they would appear as

Table 6
Optimal power dispatch of PEVs and optimal switching.

Hour	PEV fleet		Open switches
	1	2	
1	104.2342	–	s7, s12,s8,s36,s37
2	180.1713	–	s33,s12,s10,s17,s37
3	387.6286	–	s33,s13,s35,s15,s37
4	407.2103	–	s33,s34,s35,s15,s37
5	496.0000	–	s6,s13,s11,s16,s37
6	0	–	s6,s13,s9,s17,s37
7	–	0	s33,s13,s11,s36,s24
8	–	292.0000	s7,s34,s35,s17,s23
9	–	292.0000	s7,s14,s35,s17,s22
10	–	–270.0822	s33,s34,s10,s15,s24
11	–	–65.3015	s33,s34,s11,s36,s37
12	–	–289.8888	s7,s13,s11,s36,s37
13	–	–81.4208	s33,s13,s35,s16,s24
14	–	–138.1040	s7,s12,s35,s16,s37
15	–	–50.7174	s7,s34,s10,s31,s37
16	–	158.0274	s33,s13,s9,s16,s23
17	0	152.7699	s33,s14,s35,s16,s37
18	–176.1823	0	s33,s34,s35,s15,s24
19	81.7057	–	s33,s34,s35,s36,s37
20	–401.3234	–	s33,s34,s35,s17,s37
21	–81.4742	–	s7,s13,s11,s36,s37
22	–11.7573	–	s33,s14,s35,s36,s37
23	0	–	s33,s12,s11,s17,s37
24	0	–	s33,s13,s35,s17,s37

additional loads in the microgrid. In fact, while PEVs can provide new opportunity for transferring energy within the network through V2G technology, the amount of energy used by them is more than the amount of energy that will be returned to the network. This is due to the energy consumption during the travel on the road as well as the internal energy loss. The lowest value of power loss is achieved for the forth scenario which is the direct result of optimal reconfiguration of feeders. During the reconfiguration process, the topology of the microgrid is changed and new power flow paths are provided that can supply loads and PEVs with lower power losses. In other words, the reconfiguration strategy reduces the network power loss as well as operation costs by changing the network power flow. These results further advocate the valuable role of reconfiguration for reducing power loss.

Finally, Fig. 9 shows the maximum voltage deviation of buses from 1 per unit for 24 h of scheduling. According to this figure, the maximum voltage deviation of 0.1 is satisfied in all scenarios at all hours of the day successfully.

6. Conclusion

This paper investigated the optimal scheduling problem of RMGs considering dispatchable DGs, renewable DGs, and PEV fleets. First, the problem was formulated in the form of a constrained discrete single-objective optimization problem and then an efficient stochastic optimization framework was introduced to model the uncertainty effects. In order to examine the performance of the proposed stochastic framework, an IEEE test system was used and four scenarios were developed to highlight the effect of DERs, PEVs, and reconfiguration. The simulation results on a typical RMG showed that considering reconfiguration strategy can improve the microgrid's viability from both operation costs and reliability perspectives. Also, it was seen that considering the V2G technology could enhance the status of PEVs from being just loads to moving storages and thus reduce the microgrid operation cost. In other words, reconfiguration can potentially modify network power flow such that the total power loss and operation costs are reduced. In
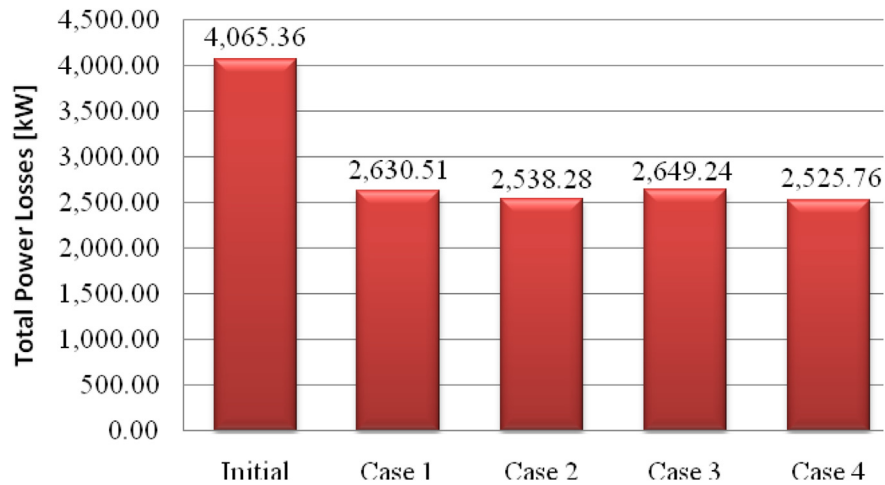
Table 5
Optimal power dispatch of DGs considering PEV and reconfiguration (kW).

DG optimal output power					
WT-1	WT-2	PV	FC	MT-1	MT-2
178.5	214.2	0	0	0	0
178.5	214.2	0	0	0	0
178.5	214.2	0	0	0	0
178.5	214.2	0	0	0	0
178.5	214.2	0	0	0	0
91.5	109.8	0	0	0	0
178.5	214.2	0	0	0	0
130.5	156.6	16	0	0	0
178.5	214.2	300	967.8	568.7	1485.8
309.0	370.8	602	594.7	289.4	1474.8
577.5	693.0	836	512.6	283.5	812.5
591.0	709.2	956	457.3	526.5	363.5
391.5	469.8	1112	273.4	1282.6	0
237.0	284.4	1084	981.6	0	756.5
178.5	214.2	630	633.5	967.4	738.5
130.5	156.6	338	987.6	759.7	1008.2
178.5	214.2	44	995.9	653.5	1368.8
178.5	214.2	0	1000	0	0
130.2	156.24	0	1000	0	0
178.5	214.2	0	1000	0	0325.4
130.05	156.06	0	1000	931.0	1497.9
130.05	156.06	0	923.8	745.0	1500.0
91.5	109.8	0	0	0	0
61.5	73.8	0	0	0	0

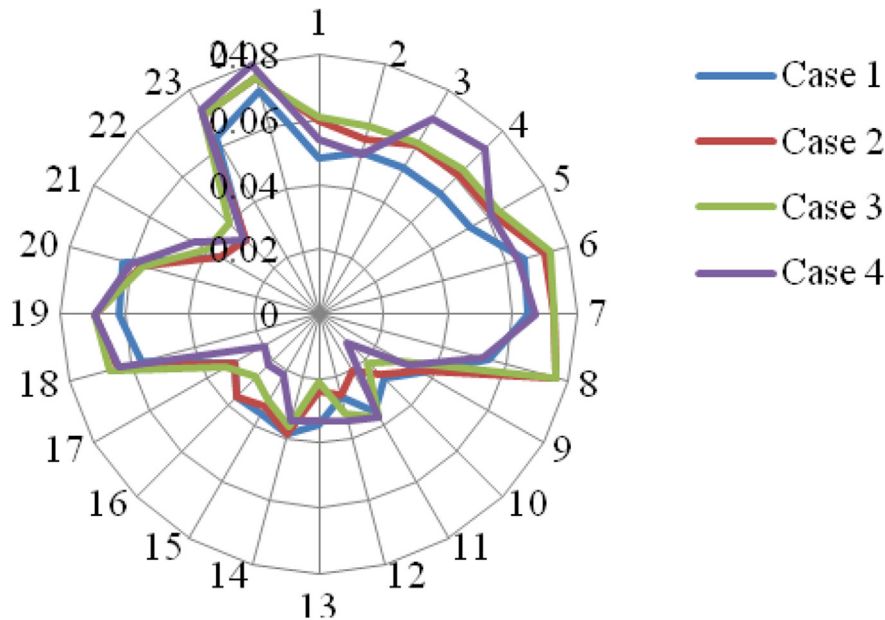**Fig. 8.** Comparison of total power losses for different cases.

Fig. 9. Maximum voltage deviation of buses in different cases.

addition, it was seen that using RESs can help the system to support local loads more reliably. Last but not least, the proposed cost function can increase the microgrid capability in supporting the renewable DGs as well as PEVs in emerging modern power grids. The follow on research of this work will focus on the stochastic operation of reconfiguration microgrids in a correlated environments, along with the assessment of dynamic preventive/corrective network reconfiguration.

References

[1] Apostolopoulou D, Bahramirad S, Khodaei A. The interface of power: moving toward distribution system operators. IEEE Power Energy Mag 2016;14(3): 46–51.
[2] Khodaei A. Resiliency-oriented microgrid optimal scheduling. IEEE Trans Smart Grid 2014;5:1584–91.
[3] Dimitrova Z, Maréchal F. Techno-economic design of hybrid electric vehicles using multi objective optimization techniques. Energy 2015;91:630–44.
[4] Kavousi-Fard A, Abunasri A, Zare A, Hoseinzadeh R. Impact of plug-in hybrid electric vehicles charging demand on the optimal energy management of renewable micro-grids. Energy 2014;78:904–15.
[5] Khodaei A. Microgrid optimal scheduling with multi-period islanding constraints. IEEE Trans Power Syst 2014;29(3):1383–92.
[6] Parhizi S, Lotfi H, Khodaei A, Bahramirad S. State of the art in research on microgrids: a review. IEEE Access 2015:890–925.
[7] Kavousi-Fard A, Niknam T. Multi-objective stochastic distribution feeder reconfiguration from the reliability point of view. Energy 2014;64:342–54.
[8] Hernandez-Aramburo C, Green TC, Mugniot N. Fuel consumption minimization of a microgrid. IEEE Trans Ind Appl 2005;41:671–81.
[9] Noori Mehdi, Gardner Stephanie, Tatari Omer. Electric vehicle cost, emissions, and water footprint in the United States: development of a regional optimization model. Energy 2015;89:610–25.
[10] Kavousi-Fard A, Khodaei A. Multi-objective optimal operation of smart reconfigurable distribution grids. AIMS Energy 2016;4(2):206–21.
[11] Arasteh H, Sadegh Sepasian M, Vahidinasab V. An aggregated model for coordinated planning and reconfiguration of electric distribution networks. Energy 2016;94:786–98.
[12] Morton AB, Mareels IMY. An efficient brute-force solution to the network reconfiguration problem. IEEE Trans Power Del 2000;15:996–1000.
[13] Kim H, Ko Y, Jung KH. Artificial neural-network based feeder reconfiguration for loss reduction in distribution systems. IEEE Trans Power Del 1993;8: 1356–66.
[14] Goswami SK, Basu SK. A new algorithm for the reconfiguration of distribution feeders for loss minimization. IEEE Trans Power Del 1992;7:1484–91.
[15] Lopez E, Opaso H. Online reconfiguration considering variability demand.

Applications to real networks. IEEE Trans Power Syst 2004;19:549—53.

[16] Taylor T, Lubkeman D. Implementation of heuristic search strategies for distribution feeder reconfiguration. IEEE Trans Power Del 1990;5:239—45.

[17] Su CT, Chang CF, Chiou JP. Distribution network reconfiguration for loss reduction by ant colony search algorithm. Electr Power Syst Res 2005;75:190—9.

[18] Chang CF. Reconfiguration and capacitor placement for loss reduction of distribution systems by ant colony search algorithm. IEEE Trans Power Syst 2008;23:1747—55.

[19] Kashem MA, Ganapathy V, Jasmon GB. Network reconfiguration for load balancing in distribution networks. Proc Inst Elect Eng Gener Transm Distrib 1999;14:563—7.

[20] Kavousi-Fard A, Niknam T, Fotuhi-Firuzabad M. A novel stochastic framework based on cloud theory and θ-modified bat algorithm to solve the distribution feeder reconfiguration. IEEE Trans Smart Grid 2015;7(2):740—50.

[21] Khodaei A. Provisional microgrids. IEEE Trans Smart Grid 2015;6(3):1107—15.

[22] Kavousi-Fard A, Niknam T. Optimal distribution feeder reconfiguration for reliability improvement considering uncertainty. IEEE Trans Power Deliv 2014;29:1344—53.

[23] Khodaei A, Bahramirad S, Shahidehpour M. Microgrid planning under uncertainty. IEEE Trans Power Syst 2015;30(5):2417—25.

[24] Zhan X, Xiang T, Chen H, Zhou B, Yang Z. Vulnerability assessment and reconfiguration of microgrid through search vector artificial physics optimization algorithm. Electr Power Energy Syst 2014;62:679—88.

[25] Dall'Anese E, Giannakis GB. Risk-constrained microgrid reconfiguration using group sparsity. IEEE Trans Sust Energy 2014;5:1415—25.

[26] Xiong J, Zhang K, Guo Y, Su W. Investigate the impacts of PEV charging facilities on integrated electric distribution system and electrified transportation system. IEEE Trans Transp Electr 2015;1:178—87.

[27] Kavousi-Fard A, Niknam T, Fotuhi-Firuzabad M. Stochastic reconfiguration and optimal coordination of V2G plug-in electric vehicles considering correlated wind power generation. IEEE Trans Sustain Energy 2015;6(3):822—30.

[28] Commission plans legislative framework to ensure the EU meets its target for cutting CO emissions from cars. Brussels: Belgium; Feb. 2007. IP/071155.

[29] Shahidinejad S, Filizadeh S, Bibeau E. Profile of charging load on the grid due to plug-in vehicles. IEEE Trans Smart Grid Mar. 2012;3(1):135—41.

[30] Yung-Tang Liao L, Chan-Nan Lu L. Dispatch of EV charging station energy resources for sustainable mobility. IEEE Trans Transp Electr 2015;1:86—93.

[31] C. Roe, A. P. Meliopoulos, J. Meisel, and T Overbye. Power system level impacts of plug-in hybrid electric vehicles using simulation data. in Proc. IEEE energy 2030, Atlanta, GA, Nov. 17—18, 2008.

[32] Dallinger D, Link J, Büttner M. Smart grid agent: plug-in electric vehicle. IEEE Trans Sustain Energy 2014;5:710—7.

[33] Even S. Graph algorithms. second ed. Cambridge University Press; 2011. p. 46—8.

[34] Lei W, Shahidehpour M, Tao L. Stochastic security-constrained unit commitment. IEEE Trans Power Syst 2007;22:800—11.

[35] Baran ME, Wu FF. Network reconfiguration in distribution systems for loss reduction and load balancing. IEEE Trans Power Deliv 1989;4:1401—7.

[36] Book. In: Soylu Seref, editor. Electric vehicles — the benefits and barriers. InTech; 2011, ISBN 978-953-307-287-6. p. 252. September 06.

[37] Golshanavaz S, Afsharnia S, Aminifar F. Smart distribution grid: optimal day-ahead scheduling with reconfigurable topology. IEEE Trans Smart Grid 2014;5:2402—11.